Scattering phase function of bullet-rosette ice crystals

Jean Iaquinta, Harumi Isaka, Pascal Personne

Scattering Phase Function of Bullet Rosette Ice Crystals

JEAN IAQUINTA, HARUMI ISAKA, AND PASCAL PERSONNE

Laboratoire de Météorologie Physique, Université Blaise Pascal, Clermont-Ferrand, France

(Manuscript received 29 March 1994, in final form 14 October 1994)

ABSTRACT

Ice crystals in cirrus frequently exhibit the shape of a bullet rosette composed of multiple bullets that radiate from a junction center. The scattering phase function of these ice crystals, pertinent to the radiation budget of cirrus, may differ from the one obtained for ice crystals with a simple geometrical shape. In this paper, the authors studied the sensitivity of the scattering phase function of a bullet rosette to its geometrical characteristics: the shape, aspect ratio, and spatial orientation. In doing so, they defined first an idealized bullet rosette according to the current knowledge of the crystalline structure and nucleation process of bullet rosettes. The scattering phase function was computed with a ray-tracing method.

The scattering phase function of a bullet rosette varies with its shape, and the lateral and backward scattering tends to increase with the number of bullets/bullet rosettes. This is due to the interaction of light scattered by a bullet with its adjacent bullets. This feature qualitatively agrees with the earlier experimental results reported for irregularly shaped particles. However, for a bullet rosette with 3D random orientation, the effect of this interaction is much smaller than expected. The normalized scattering phase function locally differs only by about 20% from one shape to another.

Earlier studies were made for ice crystals randomly oriented in a 3D space, and in this case, the scattering properties have been represented by 1D phase functions (versus the scattering angle). For a bullet rosette with preferred orientation, the scattering pattern (which is not azimuthally symmetrical and so depends on scattering angles in the 3D space) varies significantly with the shape of the bullet rosette and the direction of incident light.

Although the shape of a bullet rosette with 3D random orientation does not greatly affect the general feature of normalized scattering phase functions, its geometrical shape still remains an important factor for scattering and microphysical properties of cirrus. This is due to the fact that the geometrical cross section of a bullet rosette, perpendicular to the incident light, changes with its shape. Thus, optical properties such as the extinction coefficient of cirrus with a given ice water content may change significantly with the ice crystal shape.

1. Introduction

Cirrus is seen at all latitudes; it covers regularly about 20% of the terrestrial surface (Bretherton and Suomi 1983) and occurs frequently in all seasons (Wylie and Menzel 1989). It is considered one of the important factors controlling the radiation budget of the earth's atmosphere (Liou 1986). Microphysical and optical properties of cirrus were not yet completely understood because of its high location. In recent years, field observation programs such as FIRE (Bretherton and Suomi 1983) and ICE (Raschke et al. 1990) were carried out to collect a comprehensive set of in situ data on cirrus and to investigate relationships between its microphysical and optical properties.

The scattering behavior of ice crystals in cirrus is highly important to the radiation budget of cirrus. Many physicists (Wendling et al. 1979; Coleman and Liou 1981; Caï and Liou 1982; Takano and Jayaweera 1985; Takano and Liou 1989) have computed the scattering phase function of ice crystals with a simple geometrical shape like hexagonal plate or column. However, the ice crystals in cirrus exhibit a more complex form. Clusters of hexagonal columns or bullet rosettes were frequently observed in cirrus (Weickmann 1948); this finding was confirmed by recent observations with an airborne or balloon-borne replicator of ice crystals (Heymsfield and Knollenberg 1972; Miloshevich et al. 1992) or with a holographic camera (P. Brown 1991, personal communication; Krupp 1992). Clusters of more than eight bullets were observed in natural clouds (P. Brown 1991, personal communication) or were produced in laboratory experiments (Sato and Kikuchi 1983). The scattering phase function of these ice crystals is expected to differ from that of ice crystals with simple geometrical forms, since adjacent bullets can scatter light emerging from one of the elementary bullets that compose a bullet rosette. Zerull et al. (1980) reported that the scattering pattern of irregularly shaped particles differs significantly from the one expected for a simple convex particle, as irregular particles scatter more light

Corresponding author address: Dr. Jean Iaquinta, Laboratoire de Météorologie Physique, URA 267/CNRS, Université Blaise Pascal, 24 avenue des Landais, 63177 Aubiere cedex, France.

into the lateral direction than simple geometrical forms. On the other hand, a recent work by Macke (1993), using a simple aggregate of bullets, showed that the single-scattering phase function of these particles (similar to bullet rosettes) is basically the same as that of their individual components.

The purpose of the present study is to compute the scattering phase function of bullet rosettes by using a ray-tracing method and to investigate its sensitivity to the shape and spatial arrangement of bullets. It may help to evaluate the importance of the crystal shape for a study of optical characteristics of cirrus. Such a study would also be useful to answer a question about what microphysical parameters are important to optical properties of cirrus. Consequently, it would allow us to gain insight on how in situ microphysical data should be processed.

2. A geometrical model of the bullet rosette

Bullet rosettes were collected and observed aboard aircraft, but their geometrical characteristics were mainly reported from ground-based observations (Lee 1972; Kobayashi et al. 1976; Uyeda and Kikuchi 1979; Kobayashi 1980). The angle between the *c* axes of two adjacent bullets was found to be of 70°, or its complement of 110° for 74% of the observed crystals. Other values of the angle (40°, 55°, and 90°) were reported, respectively, for 4%, 10%, and 10% of the cases; the angle could not be determined for the remaining 2%. According to Uyeda and Kikuchi (1979, 1982), two bullets connected with the angle of 70° or 40° between their *c* axes had an *a* axis in common, while those with the angle of 55° or 90° had no common *a* axis. These frequencies of occurrence suggest that the 70° intersection corresponds to a principal mechanism of ice crystal junction and the other angles to secondary ones.

Magono (1968), Magono and Aburakawa (1968), and Parungo and Weickmann (1973) set forth the idea that a polycrystalline crystal, such as spatial dendrites and bullet rosettes, grew out from a polycrystallized supercooled droplet. Uyeda and Kikuchi (1976) experimentally determined the number of crystals in polycrystallized droplets and the angle between the *c* axes of adjacent crystals as a function of the cooling rate and droplet size. They found that the angle between adjacent crystal components had a peak frequency around 70°. According to Takahashi (1982), a bullet rosette would result from the nucleation of a cubic critical ice embryo and the subsequent growth of hexagonal columns on its (111) planes. A cubic ice embryo would explain remarkably well the 70° intersection of penetrating hexagonal columns. Whalley (1981) and Weinheimer and Knight (1987) also discussed the existence of cubic ice crystals in natural cirrus concerning Scheiner's halo (≈28°). The 40°, 55°, and 90° junctions may result from the occurrence of a repeated cubic–hexagonal junction on coincidence site lattice (CSL) during the subsequent growth of ice (Furukawa 1982; Uyeda and Kikuchi 1982).

To compute their scattering phase function, we need to choose a geometrical model for bullet rosettes: an aggregate of randomly oriented bullets or an aggregate of regularly arranged bullets. Precise knowledge on the nucleation and growth mechanisms of ice, which underlie the form of natural bullet rosettes, does not really matter as far as the angle between neighboring bullets is saved. So, we defined a simple geometrical model of bullet rosettes based on the cubic embryo assumption. This geometrical model was previously used to develop and validate a new method of classification of ice crystal pictures obtained with a Particle Measuring System (PMS) 2D probe in cirrus (Isaka et al. 1993). For simplicity, we defined an elementary single bullet as shown in Fig. 1.

This elementary bullet has 10 faces instead of 8 faces for a hexagonal column. It differs from the one adopted by Tricker in his paper about halos of unusual radii (Tricker 1979). He assumed an ice crystal with a 6-faced pyramidal end in which each pyramidal face makes an angle of inclination of 28° with its *c* axis; this pyramidal end cannot be fit to form a multibranched bullet rosette. The sharp tip of natural bullets, alone or in combinations, was explained by preferential evaporation at a junction boundary between two crystalline domains (Kobayashi 1980). Sato and Kikuchi (1983) experimentally showed the transformation of combinations of hexagonal columns formed in a cold chamber into bullet rosettes by the evaporation process. So, the trilateral pyramidal end we assumed is only an idealized form of the sharp end of natural ice crystals. Nevertheless, we decided to use this elementary bullet, because a bullet rosette of different configurations can

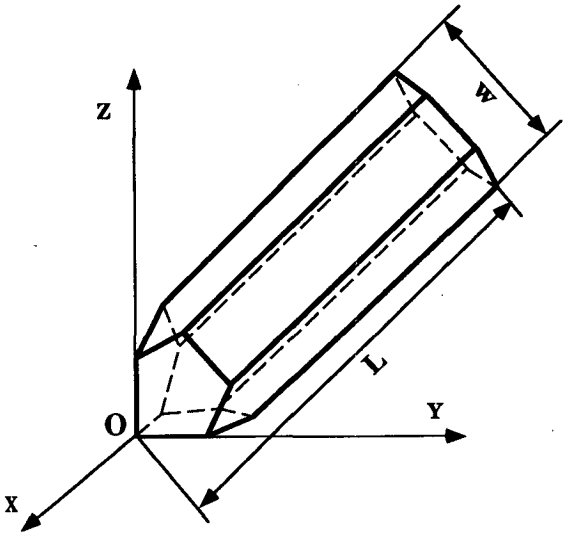

FIG. 1. Schematic representation of an elementary single bullet (L: length, w: width).

be easily formed by assembling elementary bullets either by a ridge or by a pentagonal face or even by a single point. Figure 2 shows 19 possible configurations of the bullet and bullet rosette formed by assembling 1 to 8 bullets.

3. Computation of the scattering phase function

Various methods have been developed for the computation of the single-scattering phase function of nonspherical particles—among them, anomalous diffraction theory (van de Hulst 1957; Chylek and Klett 1991), discrete dipole approximation (Flatau et al. 1988; Maslowska et al. 1994), or the Monte Carlo/geometric ray tracing. We have chosen this last method for our study, because it is straightforward to implement. The principle of a ray-tracing method is that separate rays of light hit a crystal and travel along straight lines, independently from one another (Liou and Hansen 1971). A bullet rosette was supposed to have the same optical properties in its different parts. Natural ice crystals often show surface irregularities that distribute light around the direction of specular reflection, while a smooth surface reflects only in the specular direction (Mukai et al. 1980), and another study (Macke and Tzschichholz 1992) showed that two-dimensional fractal particles provide very smooth scattering phase functions. In this study, however, we assumed a smooth crystal surface as was usually done in most of the earlier studies.

A ray hitting the smooth surface is partially reflected and refracted. The refracted light may emerge out of the crystal by another refraction, directly or possibly after several internal reflections. The absorption in ice was neglected in this study. The effect of interference was also neglected, because it only takes place when the optical pathlengths of two rays scattered in the same direction are very close to each other, which rarely happens.

Since the principle of the ray-tracing method was often given in detail in the above-cited papers, we give only a brief description of the method. The shape of a crystal is defined by its corners in a Cartesian coordinate system, and the light is incident along the z axis, perpendicular to the x–y plane. The incoming wave is represented by the two electric field components ($E^i_\perp$ and $E^i_\parallel$) that are, respectively, perpendicular and parallel to an arbitrary reference plane defined with respect to the incident beam.

Each time a ray reaches an interface between two mediums with refractive indexes n_1 and n_2, we compute the intersection point and the normal vector to the interface. The plane defined by the incident ray and the vector normal to the surface of the crystal is the incident plane. In this incident plane, the directions of the reflected and refracted rays are specified by the law of specular reflection and Snell's law (Glassner 1989). The amplitudes of the reflected ($E^r_\perp$ and $E^r_\parallel$) and refracted ($E^t_\perp$ and $E^t_\parallel$) components are given by Fresnel equations:

$$r_\perp \equiv \frac{E^r_\perp}{E^i_\perp} = \left(\frac{n_1 \cos i - n_2 \cos r}{n_1 \cos i + n_2 \cos r}\right)$$

$$t_\perp \equiv \frac{E^t_\perp}{E^i_\perp} = \left(\frac{2n_1 \cos i}{n_1 \cos i + n_2 \cos r}\right)$$

$$r_\parallel \equiv \frac{E^r_\parallel}{E^i_\parallel} = \left(\frac{n_2 \cos i - n_1 \cos r}{n_2 \cos i + n_1 \cos r}\right)$$

$$t_\parallel \equiv \frac{E^t_\parallel}{E^i_\parallel} = \left(\frac{2n_1 \cos i}{n_2 \cos i + n_1 \cos r}\right),$$

where i and r are, respectively, the angle of incidence and refraction (Born and Wolf 1991). They have to satisfy the relation $n_1 \sin i = n_2 \sin r$. The reflectance (R) is defined as the ratio of the reflected to the incident fluxes and the transmittance (T) as the ratio of the transmitted to the incident fluxes. They are given by

$$R = \left(\frac{E^r}{E^i}\right)^2 = (r_\perp \cos\varphi)^2 + (r_\parallel \sin\varphi)^2$$

$$T = \left(\frac{n_2 \cos r}{n_1 \cos i}\right)\left(\frac{E^t}{E^i}\right)^2$$

$$= \left(\frac{n_2 \cos r}{n_1 \cos i}\right)\{(t_\perp \cos\varphi)^2 + (t_\parallel \sin\varphi)^2\},$$

where φ is the angle between the polarization and incidence planes.

We followed an internally reflected ray until it carried less than 1% of the initial energy. A ray will emerge out of an ice prism only if its angle is less than 100°. Since the angle of 120° between two adjacent lateral faces of a hexagonal column is larger than 100°, a refracted ray hitting internally an adjacent crystal surface can be totally reflected and trapped; a possible exit is by one of the basal or pyramidal faces. Thus, the ray can undergo multiple internal reflections and pass from a bullet to another as shown in Fig. 3.

Diffraction is a deviation of the light ray from its rectilinear trajectory that can be explained neither by reflection nor by refraction. This departure from the geometrical optics is difficult to implement for three-dimensional objects such as a bullet rosette. Takano and Asano (1983) approximated the diffraction of hexagonal cylinders by that of spheroids of the same aspect ratio and formulated it explicitly. This is not possible for bullet rosettes, and because of the complicated shape, a ray diffracted by an elementary bullet can hit an adjacent bullet located on the far side of the first bullet. We neglected here such interaction of the diffracted light with adjacent bullets and computed the diffraction pattern due to a two-dimensional shadow of the bullet rosette.

According to Babinet's principle, the distribution of light intensity diffracted by an object is identical to that

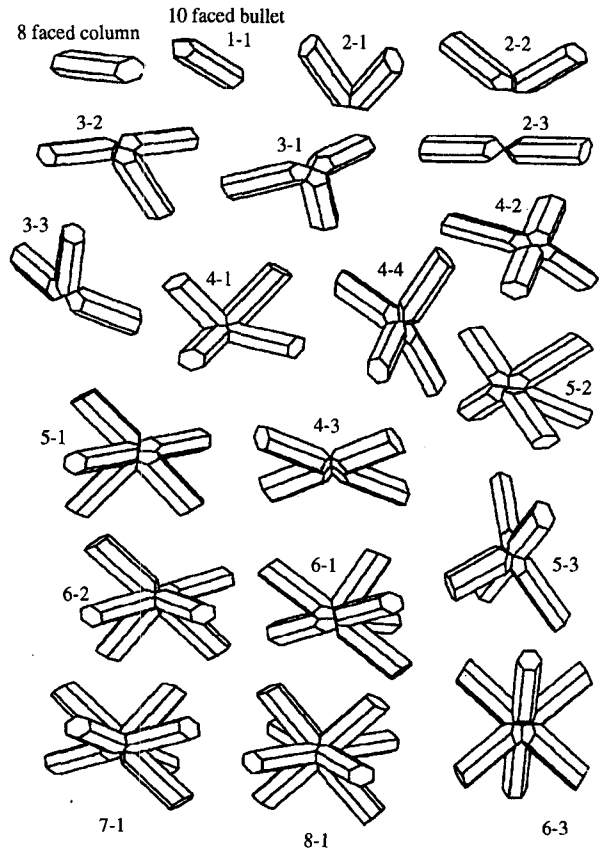

FIG. 2. The 19 configurations of the bullet rosettes generated from a cubic embryo.

by an aperture corresponding to its two-dimensional projection perpendicular to the incident beam. Diffracted energy is equal to that of the incident light on the cross section of the particle. The diffraction pattern in the far field is determined as the Fraunhofer limit. The amplitude of diffracted light by an aperture (Σ) at an arbitrary point $P(\theta, \phi)$ is given by (Born and Wolf 1991)

$$e(\theta, \phi) = Ke^{j\omega t} \int_{\Sigma} e^{-j\frac{2\pi}{\lambda}(x\cos\phi + y\sin\phi)\sin\theta} d\Sigma,$$

where

K	a coefficient of proportionality
j	the complex unit ($j^2 = -1$)
ω	the wavenumber ($2\pi/\lambda$)
θ	the scattering angle
ϕ	the azimuth angle
Σ	the area of the projected surface of the crystal
(x, y)	the coordinates of a surface element $d\Sigma$.

After an integration over the azimuth angle between 0 and 2π, we obtain

$$E(\theta) = Ke^{j\omega t} \int_{\Sigma} 2\pi J_0\left(\frac{2\pi}{\lambda}(x^2 + y^2)^{1/2}\sin\theta'\right) d\Sigma,$$

with

$$\theta' = \cos^{-1}\left(\frac{x}{\sqrt{x^2 + y^2}}\right) - \theta,$$

where J_0 is the zero order Bessel function. The diffraction intensity is given by the squared module of the amplitude:

$$I(\theta) = |E(\theta)|^2.$$

According to Fraser (1979), a spatially random orientation cannot be expected for an ice crystal whose size is larger than about 10 μm, except in highly turbulent conditions. Most ice crystals in cirrus are larger than this critical size (Heymsfield and Knollenberg 1972), and they may fall with their preferred orientation. Thus, we computed the scattering phase function for two different orientations: 3D random orientation, and 2D random orientation in which an ice crystal is oriented with the constraint (Greenler 1991) that its cross section perpendicular to the vertical is maximal (to maximize air resistance as they fall). The later orientation was chosen to simulate the effect of the preferred orientation of bullet rosettes, since precise information about the preferred orientation of bullet rosettes was not available.

Scattered light intensity was computed for 720 equally spaced intervals of the scattering angle ranging

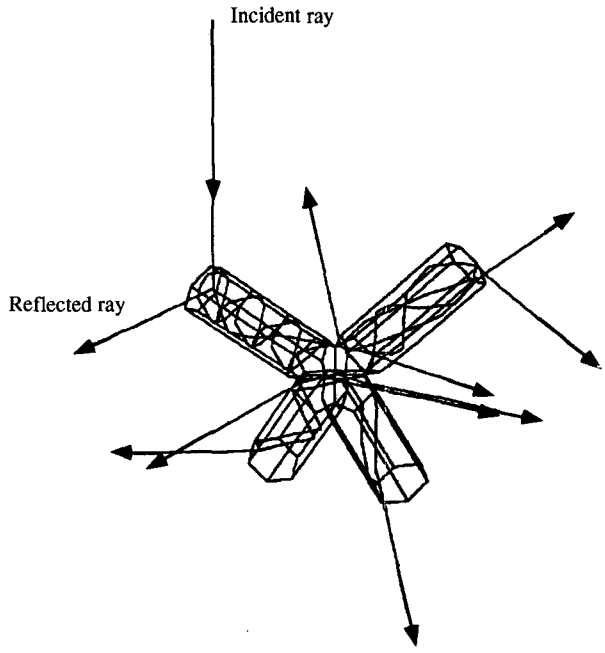

FIG. 3. An example of rays traced through a 4-branched bullet rosette (4-1 configuration).

from $\theta_0 = 0°$ to $\theta_N = 180°$ for the axisymmetrical scattering phase function. The energy of every ray with a scattering angle between θ_i and θ_{i+1} was summed up and assigned to a scattering direction $([\theta_i + \theta_{i+1}]/2)$. A total of 1×10^6 photons was used to determine an axisymmetrical scattered energy distribution. For a bullet rosette with preferred orientation, 180 equally spaced intervals for both the scattering angle and azimuthal angle were considered. Energy of every scattered ray with a scattering angle between θ_i and θ_{i+1} and an azimuthal angle between φ_j and φ_{j+1} was summed up and assigned to a scattering direction $([\theta_i + \theta_{i+1}]/2, [\varphi_j + \varphi_{j+1}]/2)$. A total of 5×10^6 photons was used to determine a scattering phase function. Up to now, the wavelength of the incident radiation was taken equal to $\lambda = 0.55$ μm, and a constant real refractive index of the ice equal to 1.31 (the imaginary part of the refractive index, $3.1 \times 10^{-9} j$ at this wavelength, was put to zero and the absorption was neglected). The refractive index of the ambient medium was assumed to be 1.0.

All the phase functions were normalized so that their integral over a spherical solid angle (4π) is equal to 1.0 [1/2 for the diffraction part and 1/2 for reflection/refraction, according to Coleman and Liou (1981)].

4. Results and discussion

a. Randomly oriented single hexagonal column and single bullet

Scattering phase functions of both a single elementary bullet and a hexagonal column of the same length (150 μm) and same aspect ratio (0.4) are represented in Fig. 4. Scattering patterns for both the shapes (hexagonal column and bullet) are characterized by a sharp peak in the direction of the incident beam (scattering angle = 0°) due to diffraction and refraction through the opposite parallel face of the ice crystal. The scattering phase function was normalized and the forward-scattering peak (of an order of 1×10^4) was not completely represented in Fig. 4. A pronounced relative peak is located at about 22° (≈21.8°) and another one at about 46° (≈45.7°). These maxima are known to be produced by light undergoing two refractions through a prism angle of, respectively, 60° and 90° (and are, respectively, the minima of deviation of the corresponding prisms, for a real refractive index of $n = 1.31$). The latter is an order of magnitude smaller than the former, because the surface area of a basal face is smaller than the surface of a prismatic side face for a hexagonal column. A broad relative maximum from 140° to 160° is produced by rays undergoing internal reflections. There is also a fairly large backscattering. Adding a sharp pyramidal end to a hexagonal column modifies the scattering pattern. The relative maxima at the angles near 22°, 46°, and 150° are recognizable with the similar amplitudes. Significant difference, due to the sharp pyramidal end of the elementary bullet, is a new peak at about 12° (≈11.5°) and another one close to 58°. The first one (12°) corresponds to two refractions through the prism angle of about 35° formed by one of the pentagonal faces and one of the side faces of the hexagonal column; the second one (58°) cannot be explained by the minimum of deviation of a prism and is due to photons that have undergone several internal reflections and that are escaping by one of the three pentagonal faces of the bullet's pyramidal end. As already mentioned, the angular relation at this sharp end is an idealized one. Thus, these peaks are entirely due to this particular angle at the pyramidal end of the elementary bullet. Nevertheless, it is noteworthy that rarely observed halos with unusual radii such as Van

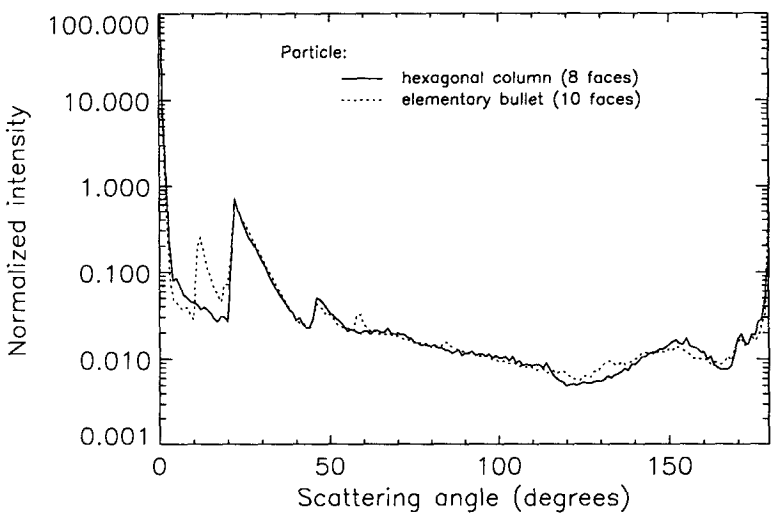

FIG. 4. Scattering phase functions of an elementary bullet and a hexagonal column ($L = 150$ μm, $w = 60$ μm).

Buijsen (8.3°), Rankin (17.4°), and Burney (19°) halos should involve one or two of the pyramidal end faces (Tricker 1979). These halos were best fitted for an inclination of a pyramidal face to the crystal axis of about 28° (Tricker 1979; Greenler 1991).

Some minor differences can also be discerned. The intensity of the 46° halo becomes smaller for a bullet than for a hexagonal column, because the effective surface of the prism angle of 90° is smaller for the bullet than for the hexagonal column. The bullet scatters more light between 115° and 140° due to internal reflection on pentagonal faces, while it scatters less for both forward-scattering angles (<5°) and backward-scattering angles (>140°).

b. *Randomly oriented bullet rosettes with multiple bullets*

To evaluate the effect of the number of bullets/bullet rosettes on the scattering phase function, we computed the scattering phase function for bullet rosettes with 2 to 8 bullets. In Fig. 5a, we represent the phase function, respectively, for the 4-3 and 4-4 bullet rosettes with 4 branches and the 8-1 bullet rosette with 8 branches: the scattering phase function for a single bullet is reproduced in this figure. The length and aspect ratio of the elementary bullet are, respectively, 150 μm and 0.4 as in Fig. 4. In spite of large differences in the crystal shape, the general feature of the normalized scattering phase function for a multibranched bullet rosette is almost identical to the one obtained for a single elementary bullet [this result was already pointed out by Macke (1993)]. Nevertheless, we can point out some differences. The 12° peak decreases as the number of exposed pentagonal faces decreases with the increased number of bullets/bullet rosettes. When two adjacent bullets are assembled by a pentagonal face, a ray hitting this face goes into another bullet and the interaction between neighboring columns occurs, as already shown in Fig. 3. Consequently, the light is scattered slightly more into the lateral direction ranging from 70° to 160°. No difference is noticed in the intensity of this peak between the single bullet and tetrahedral 4-4 bullet rosette. In the later configuration, the 4 elementary bullets share just a junction point so that each elementary bullet is not shadowed.

Differences between these scattering phase functions can be better shown by taking a ratio of scattered light intensity between a bullet rosette and a single elementary bullet. Three curves in Fig. 5b correspond to the 4-3 and 4-4 bullet rosettes and the 8-1 bullet rosette. The largest variation occurs around the 12° peak because of a smoothing effect by adjacent bullets joined by a pentagonal face. The increase in side scattering locally reaches 20% for a multibranched bullet rosette with an average increase of about 5%–10% for the multibranched bullet rosettes. Although each elementary bullet in the 4-4 bullet rosette exhibits its complete form, the corresponding curve shows that significant interaction between adjacent bullets occurs; for instance, the scattering intensity locally decreases by 10% to 20% in the range from 0° to 70°, while it increases by 10% to 20% in the range from 70° to 160°.

For different configurations of bullet rosettes, we calculated the asymmetry factor and fractions of light scattered into three angular ranges: forward (0°–60°), lateral (60°–120°), and backward (120°–180°) (as the assumption of adding diffraction in Fraunhoffer limit was chosen, some errors may have been introduced in the estimation of the forward-scattering peak, and so also in the computation of the relevant parameters). The corresponding values are given in Table 1. The asymmetry factor scarcely changes and remains around 0.836 for all bullet rosette configurations, while the side scattering between 60° and 120° (which is not affected by the diffraction part) increases about 5% at the expense of backscattering as the number of bullets/bullet rosettes increases from 1 to 8. Thus, the interaction between adjacent bullets increases with the number of bullets and contributes to the increase of side scattering as already seen in Fig. 5b.

c. *Effect of the aspect ratio of elementary bullet*

The interaction of scattered light with neighbor bullets may be expected to become more effective with increasing aspect ratio of the elementary bullet. In Fig. 6, we present the ratio of the scattering phase function of a bullet rosette with an aspect ratio of 0.2, 0.3, 0.4, and 0.5 with respect to the one with an aspect ratio of 0.1. The curves were given for the 4-1 bullet rosette. The 12° peak increases with the aspect ratio because the area of the pentagonal faces of the pyramidal end increases with the aspect ratio. Also, the larger the aspect ratio is, the larger the lateral and backward scattering and the smaller the asymmetry factor. Integrated scattering parameters are given for the aspect ratio from 0.1 to 0.8 in Table 2. A part of this increase in the side scattering is due to an increase in the lateral and backward scattering of the elementary bullet itself, as the values given in the parentheses show. The ratio of side scattering between the 4-1 configuration and the single bullet was calculated for four different aspect ratios; the corresponding ratios are, respectively, 0.96 (0.2), 1.04 (0.4), 1.02 (0.6), and 1.01 (0.8). These ratios indicate that the degree of interaction between neighboring bullets varies with the aspect ratio, increasing first with the aspect ratio of the elementary bullet, then tending to decrease. The way in which the degree of interaction varies, however, may be quite different from one shape to another. Its effect, though, generally remains less than 5%. The asymmetry factor of the scattering phase function of both the elementary bullet and bullet rosette decreases similarly from 0.87 to 0.78 as the aspect ratio changes from 0.2 to 0.8. The value of 0.78 is still far from a value of 0.7 proposed by Kinne

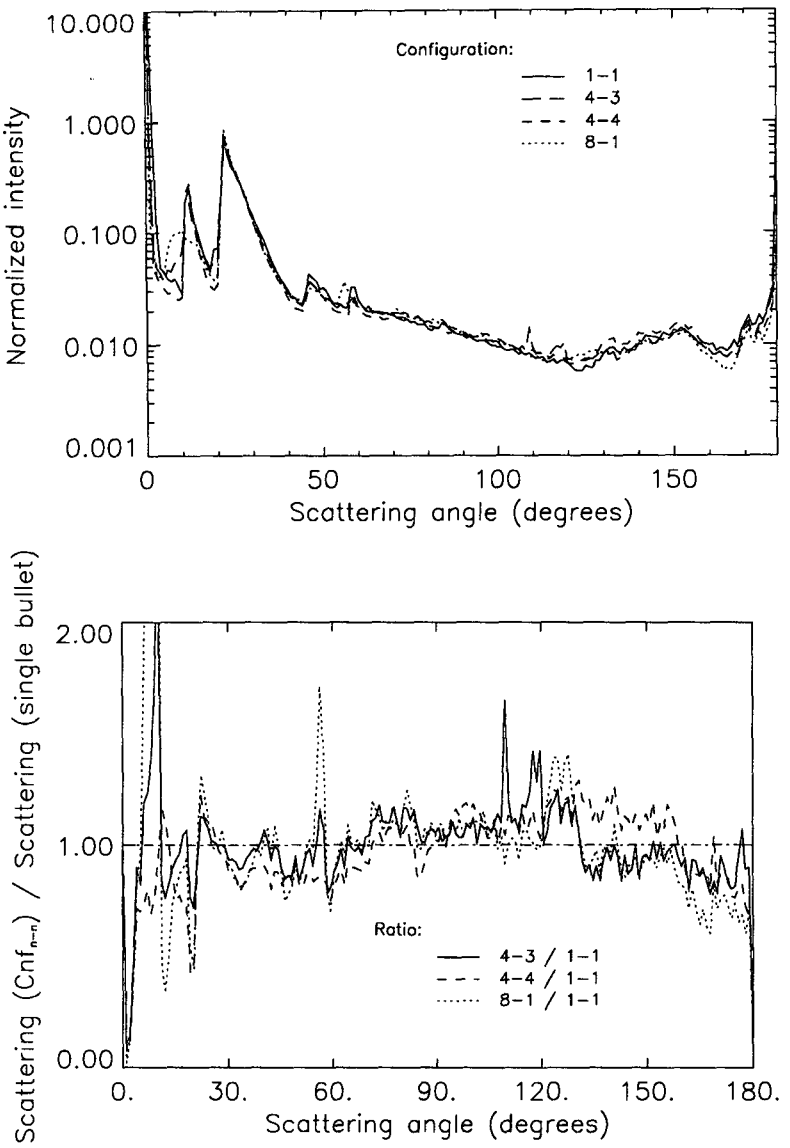

FIG. 5. (a) Scattering phase functions of multibranched bullet rosettes (L = 150 μm, w = 60 μm). (b) Variation of the ratio [scattering by a bullet rosette (configuration n-n)]/[scattering by a single bullet] with the shape of the bullet rosette (L = 150 μm, w = 60 μm).

et al. (1992) in their paper on the optical properties of cirrus clouds. So, for bullet rosettes with 3D random orientation, the effect of the number of bullets or their spatial arrangement is much less important than the effect of the aspect ratio of the single bullet.

d. Effect of preferred orientation of bullet rosettes

In the above section, ice particles were supposed to be randomly oriented in three-dimensional space. According to Fraser (1979), ice particles smaller than 20 μm in diameter can be randomly oriented by Brownian motion. In the regime of creeping flow, a particle with a simple geometrical form such as needle or thin plate can also fall without any preferred orientation (Clift et al. 1978; Happel and Brenner 1986). Ice crystals in cirrus are, however, too large to be in creeping motion or to be affected by Brownian motion. Hence, without moderate to strong turbulent motion in clouds, ice crystals would not be randomly oriented and fall rather with their preferred orientation. Some experimental studies showed that natural columnlike hexagonal ice crystals fall, for instance, with their c axis in the horizontal plane and platelike crystals with their basal plane in the horizontal plane (Ono 1969; Kajikawa 1971).

TABLE 1. Variation of integrated scattering parameters with the number of bullets/bullet rosettes (wavelength = 0.55 μm, length of elementary bullet = 150 μm, and aspect ratio = 0.4).

Bullet rosette configuration	Asymmetry factor	Energy flux (0° to 60°)	Energy flux (60° to 120°)	Energy flux (120° to 180°)
1-1	0.833	0.889	0.797×10^{-1}	0.311×10^{-1}
2-1	0.839	0.892	0.809×10^{-1}	0.272×10^{-1}
3-1	0.838	0.890	0.816×10^{-1}	0.280×10^{-1}
4-1	0.839	0.890	0.827×10^{-1}	0.270×10^{-1}
4-2	0.834	0.887	0.835×10^{-1}	0.293×10^{-1}
4-3	0.831	0.884	0.875×10^{-1}	0.286×10^{-1}
4-4	0.831	0.886	0.809×10^{-1}	0.326×10^{-1}
5-1	0.838	0.888	0.839×10^{-1}	0.277×10^{-1}
6-1	0.837	0.888	0.844×10^{-1}	0.277×10^{-1}
7-1	0.835	0.887	0.843×10^{-1}	0.284×10^{-1}
8-1	0.835	0.887	0.839×10^{-1}	0.286×10^{-1}

The scattering phase function of randomly oriented hexagonal columns with their c axis in the horizontal position was calculated (Masuda and Takashima 1989; Rockwitz 1989a,b). The scattering phase function of ice crystals in their preferred orientation differs considerably from the one determined for spatially randomly oriented hexagonal columns by the very fact that the phase function varies not only with the scattering angle, but also with the azimuth of the scattered light and the angle of the incident light. We computed the scattering phase function for hexagonal columns and also bullet rosettes in their preferred orientation. Because of lack of any precise knowledge about the preferred orientation of falling bullet rosettes, we assumed that the crystal aligned itself with its maximum cross section normal to the direction of relative motion (Clift et al. 1978; Greenler 1991). The maximum of the cross section was choosen numerically from projections over various orientations; the particles were also allowed to rotate around their vertical axis and were illuminated from a specified solar zenith angle.

The normalized scattering phase function was computed for different bullet rosettes and for various angles of the incident light. Figure 7a represents the scattering pattern for the single elementary bullet whose c axis is in the horizontal plane and that can also rotate around its c axis. Figures 7b and 7c show the scattering pattern for the 4-1 and 6-1 bullet rosettes. The length and width of the elementary bullet are 150 and 60 μm, the same as those in previous figures. In these figures, ϕ represents the angle between the incident plane and the plane defined by the scattered light and incident light, and the

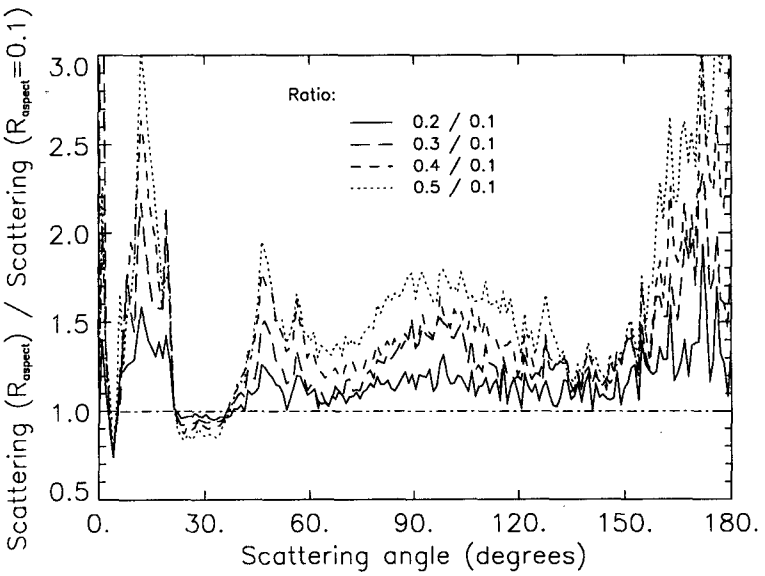

FIG. 6. Variation of the ratio [scattering by a 4-1 bullet rosette of given aspect ratio]/[scattering by the same bullet rosette of aspect ratio = 0.1] as a function of its aspect ratio (ranging from 0.2 to 0.5).

TABLE 2. Variation of integrated scattering parameters with the aspect ratio (wavelength = 0.55 μm; 4-1 bullet-rosette configuration; the numbers given in parentheses are for the single bullet with the same aspect ratio).

Aspect ratio	Asymmetry factor	Energy flux (0° to 60°)	Energy flux (60° to 120°)	Energy flux (120° to 180°)
0.1	0.876	0.918	0.619×10^{-1}	0.202×10^{-1}
0.2	0.862	0.907	0.704×10^{-1}	0.226×10^{-1}
	(0.858)	(0.903)	(0.734×10^{-1})	(0.236×10^{-1})
0.3	0.849	0.897	0.767×10^{-1}	0.260×10^{-1}
0.4	0.839	0.890	0.827×10^{-1}	0.270×10^{-1}
	(0.833)	(0.889)	(0.797×10^{-1})	(0.311×10^{-1})
0.5	0.824	0.875	0.949×10^{-1}	0.296×10^{-1}
0.6	0.809	0.862	1.047×10^{-1}	0.329×10^{-1}
	(0.804)	(0.861)	(1.031×10^{-1})	(0.358×10^{-1})
0.7	0.795	0.851	1.125×10^{-1}	0.364×10^{-1}
0.8	0.788	0.845	1.163×10^{-1}	0.384×10^{-1}
	(0.781)	(0.842)	(1.155×10^{-1})	(0.425×10^{-1})

radial distance is the angle (in linear scale) between the incident and scattered lights (θ).

For these scattering patterns, the incident plane is a plane of symmetry. They still show well-defined relative maxima of forwardly scattered light at the scattering angles of 12° and 22°. These maxima for the single bullet and bullet rosette with preferred orientation do not form closed circles of a constant intensity as would bullet rosettes with 3D random orientation. The peak of forward scattering is much broader for the 6-1 bullet rosette than the single bullet or the 4-1 bullet rosette. Compared to the forward scattering dominated by the 22° halo, the angular distribution of backwardly scattered light shows larger variation between the single bullet and multibranched bullet rosettes. This suggests that the shape of ice crystals becomes an important parameter for an analysis of bidirectional radiance data from cirrus clouds.

To evaluate globally the influence of the incident angle on the scattering by bullet rosettes with preferred orientation, we integrated the scattering phase function over two hemispheres and estimated up-

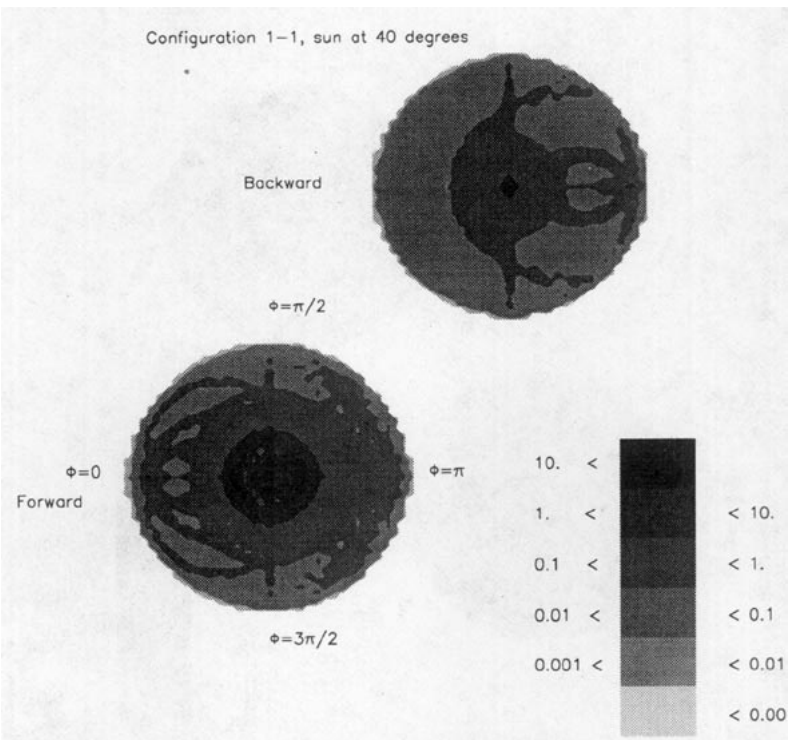

FIG. 7a. Forward- and backward-scattering patterns of a single bullet with preferred orientation (random rotation around the c axis and the vertical; the zenith angle of the incident light: 40°).

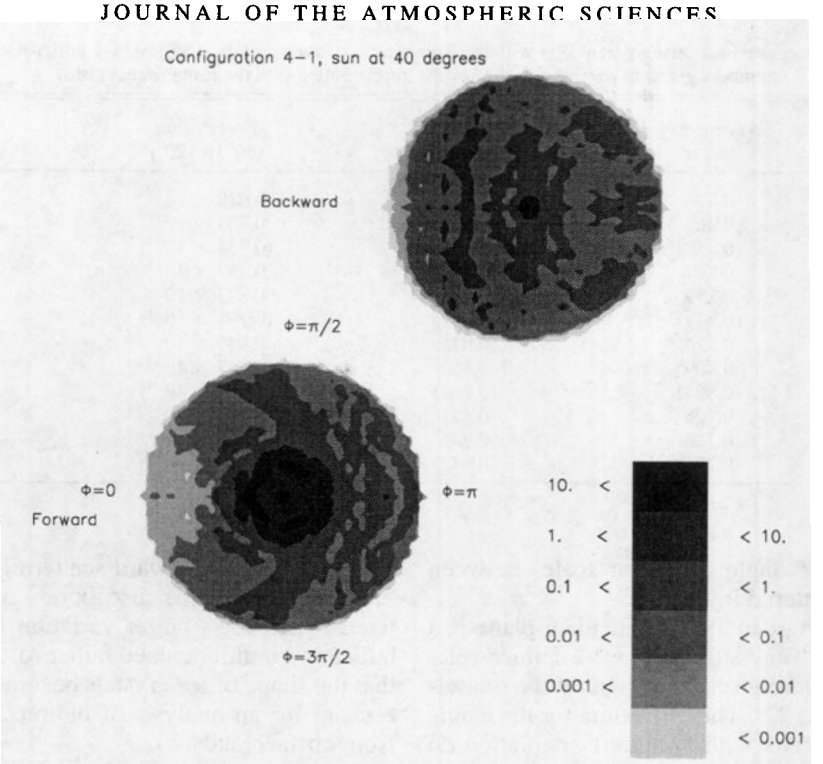

FIG. 7b. The same as in Fig. 7a but for a 4-1 bullet rosette with preferred orientation.

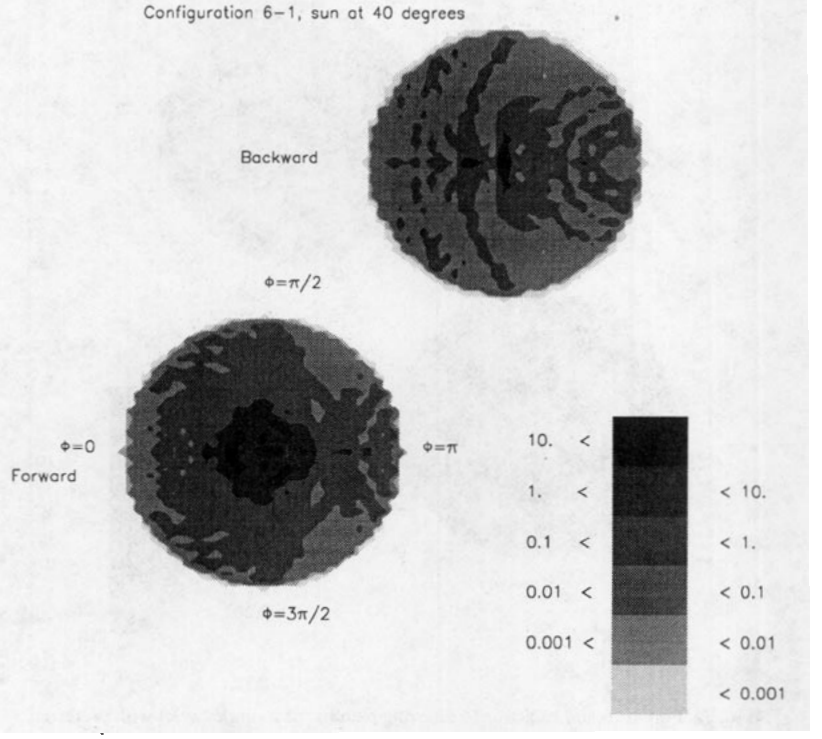

FIG. 7c. The same as in Fig. 7a but for a 6-1 bullet rosette with preferred orientation.

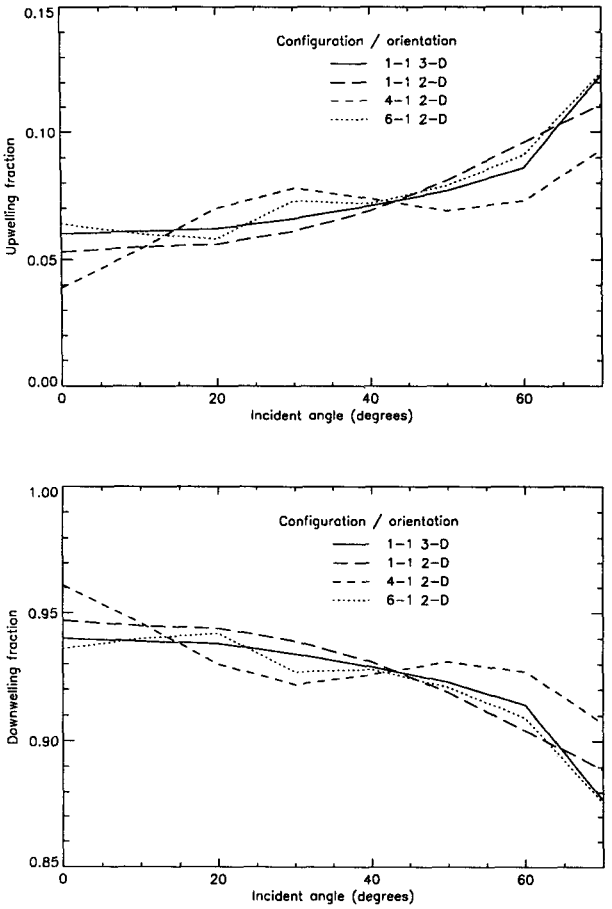

FIG. 8. (a) Upwelling fraction of scattered energy for four different bullet rosette configurations as a function of the incident angle. (b) The same as in (a) but for downwelling fraction.

welling and downwelling fractions (instead of upward and downward fluxes) of scattered light for different incident angles. Figures 8a and 8b represent the upwelling and downwelling fractions as a function of the incident zenith angle. Results were given for the single bullet and for the 4-1 and 6-1 bullet rosettes; for comparison, results for the elementary single bullet rosettes with 3D and 2D random orientations are also reproduced.

As the zenith angle of the incident light varies from 0° to 70°, the upwelling fraction of scattered light by an elementary bullet increases monotonically from 0.06 to 0.13 for 3D random orientation and from 0.05 to 0.11 for 2D random orientation. The increase is slow up to a incident angle of about 40° and rapid afterward. The variation is quite different for the 4-1 and 6-1 bullet rosettes with preferred orientation. For these cases, the upwelling and downwelling fractions show a large dependency on the shape of bullet rosette for the range of the incident angle from 0° to 50°. A relative peak of the upwelling fraction occurs around the incident angle of 30°, and it is larger than the 2D bullet case by about 20%.

e. *Probability distribution of geometrical cross section of bullet rosettes*

The above results show that the effect of crystal form on scattering phase function depends largely on the orientation of ice crystals, while the complex form of bullet rosettes has only a slight effect upon the normalized scattering pattern given that these particles are spatially randomly oriented. This raises a question of whether the form of ice crystals has any influence on radiative properties of cirrus when they are spatially randomly oriented. Indeed, if the ice crystal shape has no effect on the scattering behavior of ice crystals, and if this result in confirmed by further studies (with absorption, for various wavelengths, computation of efficiencies), there would be no need to investigate the exact shape of ice crystals in cirrus by in situ measurement. A much simpler hexagonal crystal model with variable aspect ratio might be worked out to represent microphysics in cirrus modeling and to simplify the processing of in situ microphysical data.

Figures 9a and 9b show the probability distribution of the geometrical cross section calculated for spatially randomly oriented bullet rosettes; the distributions are given for the 4-1, 4-4, 6-1, and 6-2 configurations. For the purpose of comparison, we also represent the probability distributions of the sum of 4 and 6 randomly oriented single bullets. The probability distribution changes very much with the configuration of the bullet rosette, since the shadowing effect of adjacent bullets varies from one geometrical arrangement of bullets to another and increases with the number of bullets. Thus, for the 4-4 tetrahedral configuration, the fourth bullet makes only a small contribution to the cross section, and for the bullet rosette with 6 branches, one or two branches almost always are in the shadow of other bullets and do not contribute to the cross section.

Since the scattering cross section of large ice crystals is proportional to their geometrical cross section, the total scattered energy should change significantly with the configuration and the number of bullets/bullet rosettes. The average cross section of a bullet rosette is always smaller than the average of the sum of the cross section of randomly oriented single bullets (Figs. 9a and 9b). This implies that for a given ice water content in cirrus, a population of bullet rosettes scatters less energy than a population of single bullets, provided that the aspect ratio is identical. Therefore, even if the specific configuration of randomly oriented bullet rosettes affects little its normalized scattering phase function, the scattered light intensity depends very much on the shape of ice crystals. This shape effect would also be valid for the bullet rosette with preferred orientation. In this case, the geometrical form of ice crystals induces a significant change in the normalized scattering phase

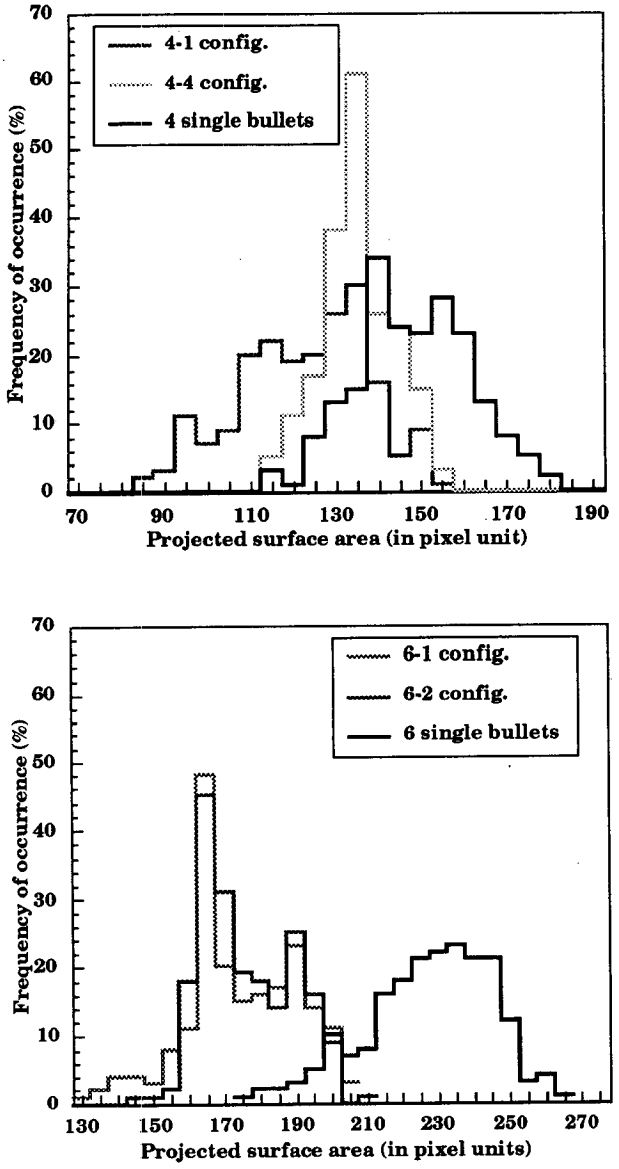

FIG. 9. (a) Probability distributions of the geometrical cross section of bullet rosettes for the 4-1 and 4-4 bullet rosettes with random orientation and the sum of cross sections of 4 single bullets with random orientation. (b) The same as in (a) but for the 6-1 and 6-2 bullet rosettes with random orientation and the sum of cross sections of 6 randomly oriented single bullets.

function as well as in their scattering cross section. The effect of the ice crystal shape on the radiative transfer will be discussed elsewhere (Chervet and Isaka 1994).

5. Conclusions

The scattering behavior of irregularly shaped bullet rosette ice crystals, observed frequently in cirrus, is one of the important factors in the relationship between radiative and microphysical properties and radiative budget of cirrus clouds. Based on the current knowledge of crystalline structure of bullet rosettes, we modeled the geometrical form of bullet rosettes as a combination of single elementary bullets. The scattering phase function of the elementary bullet is characterized by two supplementary relative maxima, respectively, at 12° and 58°, in addition to the usual peaks at 22° and 46° of a hexagonal column. The new peaks depend entirely on the pyramidal end of the single bullet we modeled. However, they still are reminiscent of some halos of unusual radii discussed by Tricker (1979).

Our study (for conservative case) shows that neither the number of bullets/bullet rosettes nor the configuration of bullet rosette affects very much the general feature of the scattering phase function given that the bullet rosettes are spatially randomly oriented. The interaction of scattering between adjacent bullets occurs, but to a degree much less than we expected. However, the increase of side scattering with the number of bullets, as well as the aspect ratio of the elementary bullet, is still significant. This tendency agrees qualitatively with experimental results obtained by Zerull et al. (1980). For bullet rosettes falling with their preferred orientation, the scattering phase function differs significantly with their configuration and the zenith angle of incident light.

Since the projected surface of n bullets constrained in a bullet rosette is not identical to the sum of projected surface of n randomly oriented single bullets, the optical and scattering properties of cirrus might be significantly affected by the geometrical form of ice crystals, even if the scattering phase function showed little influence of the crystal form. This indicates that microphysical parameters such as cross section, size, aspect ratio, apparent projected area, and form of ice crystals are all pertinent to radiative properties of cirrus. Most of these parameters can be retrieved and estimated with a specific retrieval method from PMS 2D images (Isaka et al. 1993), at least for ice crystals that can be resolved with PMS 2DC or 2DP probes. Nevertheless, further study of the form of ice crystals in cirrus and their orientation in the free atmosphere as well as in situ estimation of the scattering phase function of natural ice crystals with irregular surface is needed for better understanding of the relationship between microphysical and radiative properties of cirrus.

Acknowledgments. This work was undertaken as a part of the cooperative program ICE supported by Contract EPOC-CT90-0002.

REFERENCES

Born, M., and E. Wolf, 1991: *Principles of Optics, Electromagnetic Theory of Propagation Interference and Diffraction of Light.* 6th ed. Pergamon Press, 808 pp.

Bretherton, F. P., and V. E. Suomi, 1983: First International Satellite Cloud Climatology Project Regional Experiment (FIRE) research plan. 76 pp. [Available from the National Climatic Program Office, Rm. 108, 11400 Rockville Pike, Rockville, MD 20852.]

Caï, Q., and K. N. Liou, 1982: Polarized light scattering by hexagonal ice crystals: Theory. *Appl. Optics,* **21,** 3569–3580.

Chervet, P., and H. Isaka, 1994: Influence of crystal shape on radiance field emerging from a cirrus layer. *Contrib. Atmos. Physics,* submitted.

Chylek, P., and J. D. Klett, 1991: Absorption and scattering of electromagnetic radiation by prismatic columns: Anomalous diffraction approximation. *J. Opt. Soc. Amer. A,* **8,** 1713–1720.

Clift, R., J. R. Grace, and M. E. Weber, 1978: *Bubbles, Drops, and Particles.* Academic Press, 380 pp.

Coleman, R. F., and K. N. Liou, 1981: Light scattering by hexagonal ice crystals. *J. Atmos. Sci.,* **38,** 1260–1271.

Flatau P. J., G. L. Stephens, and B. T. Draine, 1988: Scattering on hexagonal ice crystals: Discrete dipole and anomalous diffraction approximations. *Int. Radiation Symp.,* Lille, France, Int. Assoc. Meteor. Atmos. Phys., 72–75.

Fraser, A. B., 1979: What size of ice crystals causes the halos? *J. Opt. Soc. Amer.,* **69,** 1112–1118.

Furukawa, Y., 1982: Structures and formation mechanisms of snow polycrystals. *J. Meteor. Soc. Japan,* **60,** 535–547.

Glassner, A. S., 1989: *An Introduction to Ray-Tracing.* Academic Press, 327 pp.

Greenler, R., 1991: *Rainbows, Halos, and Gories.* Cambridge University Press, 195 pp.

Happel, J., and H. Brenner, 1986: *Low Reynolds Number Hydrodynamics.* Martinus Nijhoff Publishers, 553 pp.

Heymsfield, A. J., and R. G. Knollenberg, 1972: Properties of cirrus generating cells. *J. Atmos. Sci.,* **29,** 1358–1366.

Isaka, H., J. Iaquinta, and P. Personne, 1993: Estimation of geometrical characteristics of bullet-rosettes from PMS-2D images. *J. Atmos. Oceanic Technol.,* submitted.

Kajikawa, M., 1971: A model experimental study on the falling velocity of ice crystals. *J. Meteor. Soc. Japan,* **49,** 367–375.

Kinne, S., T. P. Ackermann, A. J. Heymsfield, F. P. J. Valero, K. Sassen, and J. D. Spinhirne, 1992: Cirrus microphysics and radiative transfer: Cloud field study on 28 October 1986. *Mon. Wea. Rev.,* **120,** 661–684.

Kobayashi, T., 1980: *Rokka no Bi* (Beauty of Snow Ice Crystal). Saiensu-sha, 249 pp.

——, Y. Furukawa, K. T. Takahashi, and H. Uyeda, 1976: Cubic structure models at the junctions in polycrystalline snow crystals. *J. Cryst. Growth,* **35,** 262–267.

Krupp, C., 1992: Holographische Messungen an Eiskristallen in Cirruswolkn während des Internationalen Cirrus Experiments ICE. GKSS 92/E/14, 145 pp.

Lee, C. W., 1972: On the crystallographic orientation of spatial branches in natural polycrystalline snow crystals. *J. Meteor. Soc. Japan,* **50,** 171–179.

Liou, K. N., 1986: Influence of cirrus clouds on weather and climate processes: A global perspective. *Mon. Wea. Rev.,* **114,** 1167–1199.

——, and J. E. Hansen, 1971: Intensity and polarization for single scattering by polydisperse spheres: A comparison of ray optics and Mie theory. *J. Atmos. Sci.,* **28,** 995–1004.

Macke, A., 1993: Scattering of light by polyhedral ice cristals. *Appl. Opt.,* **32,** 2780–2788.

——, and F. Tzschichholz, 1992: Scattering of light by fractal ice particles: A qualitative estimate exemplary for two-dimensional triadic Koch-island. *Proc. 5th Workshop ICE/EUCREX,* Clermont-Ferrand, France, 159–170.

Maslowska, A., P. J. Flatau, and G. L. Stephens, 1994: On the validity of the anomalous diffraction theory to light scattering by cubes. *Opt. Commun.,* **107,** 35–40.

Magono, C., 1968: On the additional nucleation of natural snow crystals. *J. Rech. Atmos.,* **3,** 147–152.

——, and H. Aburakawa, 1968: Experimental studies on snow crystals of plane type with spatial branches. *J. Fac. Sci., Hokkaido Univ., Ser. 7,* **3,** 85–97.

Masuda, K., and T. Takashima, 1989: Numerical estimation of the effect of multiple scattering by horizontally randomly oriented hexagonal ice crystals. *Int. Radiation Symp.,* Lille, France, Int. Assoc. Meteor. Atmos. Phys., 53–56.

Miloshevich, L. M., A. J. Heymsfield, and P. M. Norris, 1992: Microphysical measurements in cirrus clouds from ice crystal replicator sondes launched during FIRE II. *Proc. 11th Int. Conf. on Clouds and Precipitation,* Montreal, Canada, Int. Comm. Clouds and Precip., Int. Assoc. Meteor. Atmos. Phys., 525–528.

Mukai, S., T. Mukai, and R. H. Giese, 1980: Scattering of radiation by a large particle with a rough surface. *Light Scattering by Irregularly Shaped Particles,* D. W. Schuerman, Ed., Plenum Press, 219–225.

Ono, A., 1969: The shape and riming properties of ice crystals in natural clouds. *J. Atmos. Sci.,* **26,** 138–147.

Parungo, F. P., and H. K. Weickmann, 1973: The growth of ice crystals from frozen cloud droplets. *Beitr. Phys. Atmos.,* **46,** 289–304.

Raschke, H., J. Schmetz, J. Heinzenberg, R. Kandel, and R. Saunders, 1990: International Cirrus Experiment. *ESA Bull.,* **14,** 113–119.

Rockwitz, K. D., 1989a: Three-dimensional scattering functions of ice crystals and depolarization effects. *Int. Radiation Symp.,* Lille, France, Int. Assoc. Meteor. Atmos. Phys., 47–49.

——, 1989b: Scattering properties of horizontally oriented ice crystal columns in cirrus clouds. Part 1. *Appl. Optics,* **28,** 4103–4110.

Sato, N., and K. Kikuchi, 1983: Artificial making of snow crystals of cold temperatures types: Progress report on the study of snow crystals of cold temperature types. *J. Fac. Sci., Hokkaido Univ.,* 81–131.

Takahashi, T., 1982: On the role of cubic structure in ice nucleation. *J. Cryst. Growth,* **59,** 441–449.

Takano, Y., and S. Asano, 1983: Fraunhofer diffraction by ice crystals suspended in the atmosphere. *J. Meteor. Soc. Japan,* **61,** 289–300.

——, and K. Jayaweera, 1985: Scattering phase matrix for hexagonal ice crystals computed from ray-tracing. *Appl. Opt.,* **24,** 3254–3263.

——, and K. N. Liou, 1989: Solar radiative transfer in cirrus clouds. Part I: Single-scattering and optical properties of hexagonal ice crystals. *J. Atmos. Sci.,* **46,** 3–19.

Tricker, R. A. R., 1979: Arcs associated with halos of unusual radii. *J. Opt. Soc. Amer.,* **69,** 1093–1100.

Uyeda, H., and K. Kikuchi, 1976: On the orientation of the principal axis of frozen water droplets. *J. Meteor. Soc. Japan,* **54,** 267–275.

——, and ——, 1979: Observations of the three dimensional configuration of snow crystals of combination of bullet type. *J. Meteor. Soc. Japan,* **57,** 488–492.

——, and ——, 1982: Some consideration of combination of bullets which have the axial angle between the c-axes of 90°. *J. Fac. Sci., Hokkaido Univ., Ser. 7,* **7,** 145–157.

van de Hulst, H., 1957: *Light Scattering by Small Particles.* Dover, 470 pp.

Weickmann, H. K., 1948: *Die Eisphase in der Atmosphäre* (The Ice Phase in the Atmosphere). Royal Aircraft Establishment, 96 pp.

Weinerheimer, A. J., and C. A. Knight, 1987: Scheiner's halo: Cubic ice or polycristalline hexagonal ice? *J. Atmos. Sci.,* **44,** 3304–3308.

Wendling, P., R. Wendling, and H. K. Weickmann, 1979: Scattering of solar radiation by hexagonal ice crystals. *Appl. Opt.,* **18,** 2663–2671.

Whalley, E., 1981: Scheiner's halo: Evidence for ice *Ic* in the atmosphere. *Science,* **211,** 389–390.

Wylie, D. P., and W. P. Menzel, 1989: Two years of cloud cover statistics using VAS. *J. Climate,* **2,** 380–392.

Zerull, R. H., R. H. Giese, S. Schwill, and K. Weiss, 1980: Scattering by particles of non-spherical shape. *Light Scattering by Irregularly Shaped Particles,* D. W. Schuerman, Ed., Plenum Press, 273–282.